Computer Assisted Mechanics and Engineering Sciences, 5: 45–54, 1998.

Shape optimization method for nozzle design

Zoran Mrša and Gorazd Medić
Technical faculty, University of Rijeka, Vukovarska 58, HR-51000 Rijeka, Croatia

(Received September 30, 1996)

The optimization of the nozzle shape was carried out using the finite element incompressible viscous flow solver, with discretization of total derivative, with the originally developed software. Optimization procedure used conjugate gradient method, with finite difference approximation of gradient of objective function. The mesh generator, specially adapted for chosen shape parametrization in the form of splines using Bezier cubic curve segments, has been used in optimal shape design of the nozzle. The examples of optimization with constraints, the nozzle shape optimization, and the unconstrained optimization of the confusor are presented. All test cases showed good convergence properties that qualifies the proposed methodology as appropriate for shape optimization in viscous flow problems.

1. INTRODUCTION

The shape optimization technique is today accepted engineering tool. It is a promising method for the engineer designer because it can supplement his experience and guide him when designing new geometry or trying to improve the efficiency of the existing one. For the simple geometry and simple flow models, such as 2D airfoils or wing profiles, the shape optimization methods are widely used, but they remain quite unused for complex configurations or complex flow models. For 2D domains and potential flow models a good theory exists for a shape optimization, Pironneau [10] and a lot of papers can be found in literature, e.g. Weeber and Hoole [14], Mrša [6], Bugeda et al. [1], Mrša and Sopta [9] and Sopta and Mrša [12]. Approach of using a cheap direct flow solver and very general robust constraint methods is accepted in 3D industrial aerodynamics design, Fol et al. [4]. A review of recent advances for modeling of aeronautical flows can be found in Dervieux [2], where genetic algorithms have been shown to be surprisingly useful tool for many optimization problems. However, reports on shape optimization for viscous flow problems are rare, although there are many cases in mechanical and civil engineering design that are subject to minimization of the energy losses of the flow around obstacles or through orifices, nozzles and like apparatus.

The finite element incompressible viscous flow solver, with discretization of total derivative, Pironneau [11], has been tested on many test cases showing good convergence properties and robustness, Mrša [7]. Optimization software with conjugate gradient optimizer and specially tailored mesh generator for chosen shape parametrization, using domain decomposition technique, originally developed by authors, has been successfully used in cases of turbomachinery spiral casing optimal shape design, with 3D potential flow model.

The aim of this work is to find optimum nozzle shape for laminar viscous flow. Mathematical model for laminar flow of incompressible viscous fluid, the boundary value problem for Navier-Stokes equations, is given in chapter two. For a numerical solution, the finite element method has been developed utilizing quadrilateral isoparametric elements. In chapter three, the application of the Galerkin weighted residual method with discretization of directional derivative of velocity is presented. The formulation of the shape optimization algorithm is given in chapter four. Using incompressible viscous flow solver and conjugate gradient method, the energy losses, defined as the difference of total mechanical energy fluxes in inflow and outflow cross-sections, are minimized in

the set of admissible nozzle shapes. The shape of the nozzle is parametrized by splines using Bezier cubic curve segments, their coefficients being optimizing parameters.

2. Mathematical model of the incompressible viscous fluid flow

The partial differential equations set governing viscous, laminar, steady, axisymmetric flow of incompressible fluid, known as Navier-Stokes equations and equation of continuity, are, Taylor and Hughes [13],

$$u\frac{\partial u}{\partial x}+v\frac{\partial u}{\partial r}=f_x-\frac{1}{\rho}\frac{\partial p}{\partial x}+\nu\left(\frac{\partial^2 u}{\partial x^2}+\frac{1}{r}\frac{\partial u}{\partial r}+\frac{\partial^2 u}{\partial r^2}\right) \quad \text{in } \Omega, \tag{1}$$

$$u\frac{\partial v}{\partial x}+v\frac{\partial v}{\partial r}=f_y-\frac{1}{\rho}\frac{\partial p}{\partial r}+\nu\left(\frac{\partial^2 v}{\partial x^2}+\frac{1}{r}\frac{\partial v}{\partial r}-\frac{v^2}{r}+\frac{\partial^2 v}{\partial r^2}\right) \quad \text{in } \Omega, \tag{2}$$

$$\frac{\partial u}{\partial x}+\frac{\partial v}{\partial r}+\frac{v}{r}=0 \quad \text{in } \Omega, \tag{3}$$

where u and v are velocity components, p pressure, f_x, f_y body force components, ν viscosity and ρ density of the fluid. The boundary conditions treated in this work are

$$(u,v)=(\hat{u},\hat{v}), \quad \text{given on } \Gamma_u, \tag{4}$$

$$\left(\frac{\partial v}{\partial n},\frac{\partial v}{\partial n}\right)=\left(\widehat{\frac{\partial u}{\partial n}},\widehat{\frac{\partial v}{\partial n}}\right) \quad \text{given on } \Gamma_n, \tag{5}$$

where $\Gamma_u \cup \Gamma_n = \partial\Omega$ is the boundary of Ω and n is the outer unit normal to the $\partial\Omega$. These equations are particularly difficult to integrate in the case of typical application, especially for small values of ν, because of the boundary layers and turbulence. Even the mathematical study of Navier–Stokes equations is not complete.

3. Finite element approximation with discretization of directional derivative

We introduce a discretization of domain as union of finite elements in the usual manner with the use of quadratic shape function and so called eight node serendipity isoparametric finite element approximation for velocity components and superparametric four node for pressure:

$$u=\sum_{i=1}^{8}N_i(\xi,\eta)u_i\,, \qquad v=\sum_{i=1}^{8}N_i(\xi,\eta)v_i\,,$$

$$x=\sum_{i=1}^{8}N_i(\xi,\eta)x_i\,, \qquad y=\sum_{i=1}^{8}N_i(\xi,\eta)y_i\,,$$

$$p=\sum_{i=1}^{4}M_i(\xi,\eta)p_i\,,$$

where

$$N_i(\xi,\eta)=\frac{1}{4}(1+\xi_i\xi)(1+\eta_i\eta)(\xi_i\xi+\eta_i\eta-1)$$

for corner nodes $i=1,3,5,7$ and for midside nodes

$$N_i(\xi,\eta)=\frac{1}{4}(1-\xi^2)(1+\eta_i\eta), \qquad \xi_i=0, \quad i=2,6,$$

$$N_i(\xi,\eta)=\frac{1}{4}(1+\xi_i\xi)(1+\eta^2), \qquad \eta_i=0, \quad i=4,8,$$

and

$$M_i(\xi,\eta) = \frac{1}{4}(1+\xi_i\xi)(1+\eta_i\eta), \qquad i = 1,3,5,7.$$

The use of lower order finite element approximation elements for pressure is to avoid the pressure solution oscillations which occurs for equal order approximation [11].

3.1. Discretization of directional derivative

Let $X(x,y,t;\tau)$ be the orbit (or the trajectory) of the flow field $w(x,y) = (u,v)$ such that

$$\frac{\mathrm{d}X(\tau)}{\mathrm{d}\tau} = w(X(\tau)), \qquad X(t) = (x,y), \tag{6}$$

Then the directional derivative of velocity becomes, Pironneau [11]:

$$(w\cdot\nabla)w = \frac{\partial}{\partial\tau}w(X(x,y,t;\tau))\bigg|_{\tau=t}, \tag{7}$$

Thus we can write

$$(w\cdot\nabla)w \cong \frac{1}{\delta}\{w(x,y) - w(X_\delta(x,y))\}, \tag{8}$$

where $X_\delta(x,y)$ is an approximation of $X(x,y,t;\tau-\delta)$. Euler scheme is chosen for approximate solution:

$$X_\delta(x,y) = x - w(x,y)\delta\,. \tag{9}$$

Euler scheme is of order $O(\delta^2)$. The equation above is solved iteratively. First w_0 is assumed. Knowing w_n, $X_\delta^{n+1} = x - w^n(x,y)\delta$ is calculated and w^{n+1} as the solution for velocity field. If the convergence test is satisfied the iteration stops, otherwise continues.

3.2. Galerkin weighted residual approach

Applying Galerkin weighted residual approach to the Navier–Stokes equations and the equation of continuity we get the system of algebraic equations

$$A\phi = b + c,$$

where

$$\phi = (u_i, p_i, v_i)^T, \qquad i = 1,2,..N_p\,,$$

$$A_{ij} = \sum_{e=1}^{N_e}\left(\int_{A^e} C\,\mathrm{d}A^e - \int_{\Gamma^e} D\,\mathrm{d}s\right),$$

where C and D are 3×3 matrices with non-zero components:

$$C_{11} = C_{33} = \frac{1}{\delta}N_j(N_j - \tilde{N}_j) + \nu\left(\frac{\partial N_i}{\partial x}\frac{\partial N_j}{\partial x} + \frac{\partial N_i}{\partial y}\frac{\partial N_j}{\partial y}\right),$$

$$C_{12} = N_i\frac{\partial M_l}{\partial x}, \qquad C_{21} = M_i\frac{\partial N_j}{\partial x}, \qquad C_{23} = M_i\frac{\partial N_j}{\partial y}, \qquad C_{32} = N_i\frac{\partial M_l}{\partial y},$$

$$D_{11} = D_{33} = \nu N_i\frac{\partial N_j}{\partial n}\,.$$

Right hand side vectors, due to body force densities and given normal derivative of the velocity, are

$$b_i = \sum_{e=1}^{N_e} \left(\int_{A^e} f \, \mathrm{d}A^e \right), \qquad c_i = \sum_{e=1}^{N_e} \left(\int_{\Gamma^e} q \, \mathrm{d}s \right),$$

where f and q are

$$f = (N_i f_x,\ 0,\ N_i f_y)^T, \qquad q = \left(\nu N_i \left. \frac{\partial u_j}{\partial n} \right|_{\Gamma_2},\ 0,\ \nu N_i \left. \frac{\partial v_j}{\partial n} \right|_{\Gamma_2} \right).$$

In the above formulas the outer summation (index e) goes over all N_e elements, N_p is the number of nodes in $\Omega \setminus \Gamma_u$, N_m is the number of midside nodes.

The shape function $\tilde{N}_j$ denotes the upstream advected shape function N_j :

$$\tilde{N}_j = N_j \circ X_\delta,$$

that is

$$\tilde{N}_j(x,y) = N_j(x - u(x,y)\delta \ , \ y - v(x,y)\delta).$$

To solve linear system the frontal method is used.

4. Geometry definition

The geometry of the nozzle is defined by spline curve with cubic Bezier curve segments in the form of

$$P_i(t) = \sum_{j=0}^{3} B_{j,3}(s)\, Q_{3(i-1)+j}\,, \qquad i = 1, 2...n, \tag{10}$$

where n denotes total number of curve segments, $B_{j,3}(s)$ is j-th Bernstein basis function

$$B_{j,3}(s) = \binom{3}{j} (1-s)^{3-j} s^j \tag{11}$$

with parameter s defined as

$$s = \frac{t - t_{i-1}}{t_i - t_{i-1}}\,,$$

where t_i are the knot values $t_0\,, t_1\,, \ldots, t_n$ of the global curve parameter t at the ends of segments. The $Q_{3(i-1)+j}$, $i = 1, \ldots n$, $j = 0, 1, 2, 3$, are $3n + 1$ curve defining vectors Q_0, $Q_1\,, \ldots Q_{3n}$, Yamaguchi [15]. The connection conditions, the continuity of the shape and curvature vectors are expressed by following system of equations:

$$\begin{aligned} &h_i(Q_{3i+1} - Q_{3i}) = h_{i+1}(Q_{3i} - Q_{3i-1}), \qquad i = 1, 2, ...n-1, \\ &Q_{3i-1} + \frac{h_{i+1}}{h_i}(Q_{3i-1} - Q_{3i-2}) = Q_{3i+1} + \frac{h_i}{h_{i+1}}(Q_{3i+1} - Q_{3i+2}), \end{aligned} \tag{12}$$

where

$$h_i = t_i - t_{i-1}\,.$$

5. FORMULATION OF THE SHAPE OPTIMIZATION ALGORITHM

The objective functional is defined as energy losses of the flow, Landau [5],

$$e = \frac{1}{2}\mu \int_{\Omega} |\nabla \mathbf{v} + \nabla \mathbf{v}^t|^2 \, \mathrm{d}V,$$

with μ dynamic viscosity coefficient, $\mathbf{v}$ velocity, that is for stationary flows equal to the difference of the energy fluxes between outflow and inflow cross-sections

$$e = e_o - e_i \,. \tag{13}$$

The energy flux through given cross-section A is defined as

$$e_A = \int_A \rho \left(\frac{u^2 + v^2}{2} + \frac{p}{\rho} + gz \right) v_n \, \mathrm{d}A \tag{14}$$

where g is gravitational acceleration, z height, and v_n normal velocity component.

The geometry of the nozzle is parametrized by $2(3n+1)$ parameters,

$$Q_{i,j} = \{Q_{i,0}\,,\ Q_{i,1}\,, \ldots,\ Q_{i,3n}\}, \qquad i = 1, 2,$$

in the form of the parametrically defined plane curve given with (10). The formulation of the nozzle shape optimization is as follows:

> Find optimum nozzle shape, i.e. $2(3n+1)$ parameters $Q_{i,j}$, $i = 1, 2$, $j = 0, \ldots, 3n$, that minimize the objective functional e, given by (13).

This problem is usually subject to constraints resulting from the conditions of specifying certain points or tangent lines of the desired curve. The convergence of conjugate gradient procedure is dependent on the smoothness of the gradient of the objective function. Therefore it should be calculated with care. Because the gradient depends on the mesh, the general mesh generator, i.e. the automatic unstructured mesh generator is not adequate, since it may change the mesh abruptly in the process of automatic meshing by adding new elements. The smooth behavior of the gradient is achieved here by specially tailored mesh generator. In the process of conjugate gradient solution, the gradient of the objective functional is approximated by finite differences.

6. NUMERICAL RESULTS

Two different cases were tested: the standard nozzle and the confusor with continuously varied cross section (Fig. 1). The starting shape of the nozzle was chosen on the basis of the standard shape given in the norm ISO 5167 (DIN 1952 [3]), and in particular the ISA 1932-nozzle suited for turbulent flow measurements with $Re > 20000$. In this analysis we have chosen $Re = 100$ (based on the nozzle opening diameter d), leading to the laminar flow regime with the flow losses due to recirculation predominant over the flow losses due to wall shear. We concentrated our attention on the optimization of the curved part of the nozzle, excluding the cylindrical afterbody from the analysis. The start and end points of the curved nozzle generatrix have been taken fixed and the starting shape was chosen as a 90 degree circular arc, leading to the opening $\beta = d/D = 0.5$ (see Fig. 1).

We used $n = 2$ curve segments in (10) to define the nozzle and confusor geometries. Fixing the start and end points and their tangents as well as the x coordinate of the middle point, using the equations (12), reduced the number of optimization parameters to 4 : x coordinate of the point Q_1, y coordinate of the point Q_3, y coordinate of the point Q_5 in the case of the nozzle and x coordinate of the point Q_5 in the case of the confusor, and ratio of the parameter intervals of the

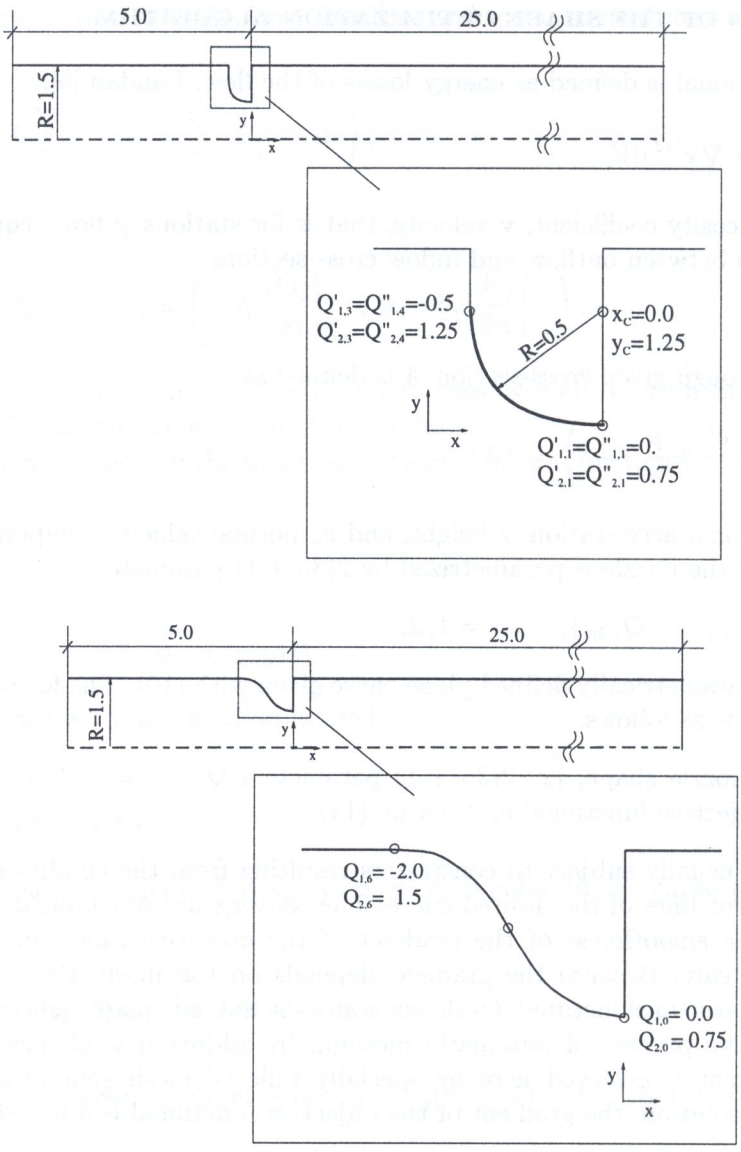

Fig. 1. The starting geometry of the nozzle and confusor

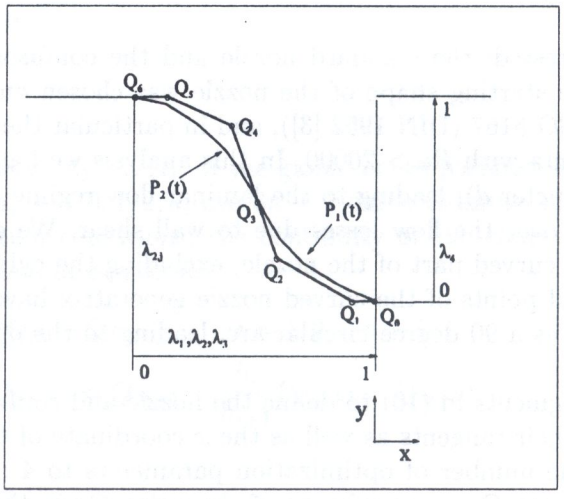

Fig. 2. The definition of optimization parameters

two Bezier segments (Fig. 2). In order to normalize parameter intervals new set of parameters is introduced:

$$
\begin{aligned}
&Q_{1,1} = (1-\lambda_1)Q_{1,6} + \lambda_1 Q_{1,0}\,, \quad && Q_{2,1} = 0.75, && \\
&Q_{2,3} = (1-\lambda_3)Q_{2,0} + \lambda_3 Q_{2,6}\,, && Q_{1,3} = 0.25, && \text{for nozzle,}\\
&Q_{2,5} = (1-\lambda_2)Q_{2,0} + \lambda_2 Q_{2,6}\,, && Q_{1,5} = 0.5\ , && \text{for nozzle,}\\
&Q_{2,3} = (1-\lambda_3)Q_{2,0} + \lambda_3 Q_{2,6}\,, && Q_{1,3} = 1.\ , && \text{for confusor,}\\
&Q_{1,5} = (1-\lambda_2)Q_{1,6} + \lambda_2 Q_{1,0}\,, && Q_{2,5} = 1.5\ , && \text{for confusor,}\\
&\frac{h_2}{h_1} = \lambda_4\,. &&&&
\end{aligned}
$$

Unconstrained shape optimization with quadratic Bezier curve segment led to the degenerated nozzle shape in the form converging to optimal confusor shape, Mrša [8]. With given fixed start and end points the shape tended to form bulb like configuration. Therefore, we constrained the nozzle axial length. Further on we used projected conjugate gradient method, Pironneau [10].

The optimal shape is given in Fig. 3. The streamlines and pressure contour on the axes of symmetry are plotted in Figs. 4 and 5. The inflow to outflow cross-section pressure drop is the measure of the flow losses, since the velocity profile recovers almost completely at the outflow boundary.

The optimal nozzle shape parameters and objective functional value are given in Table 1.

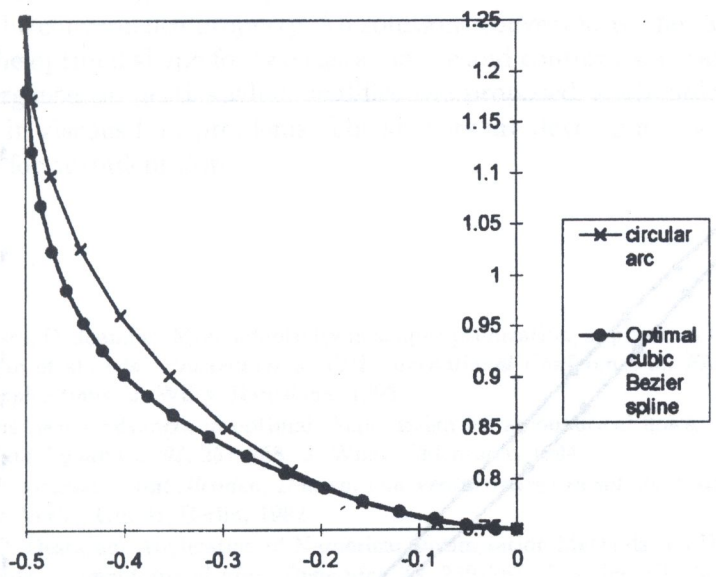

Fig. 3. Optimal nozzle shape

Fig. 4. Streamlines for optimal nozzle shape

Table 1. The optimal nozzle shape parameters (λ_i) and functional value e

λ_1	λ_2	λ_3	λ_4	e
0.8628	0.5063	0.2278	1.3115	59.014

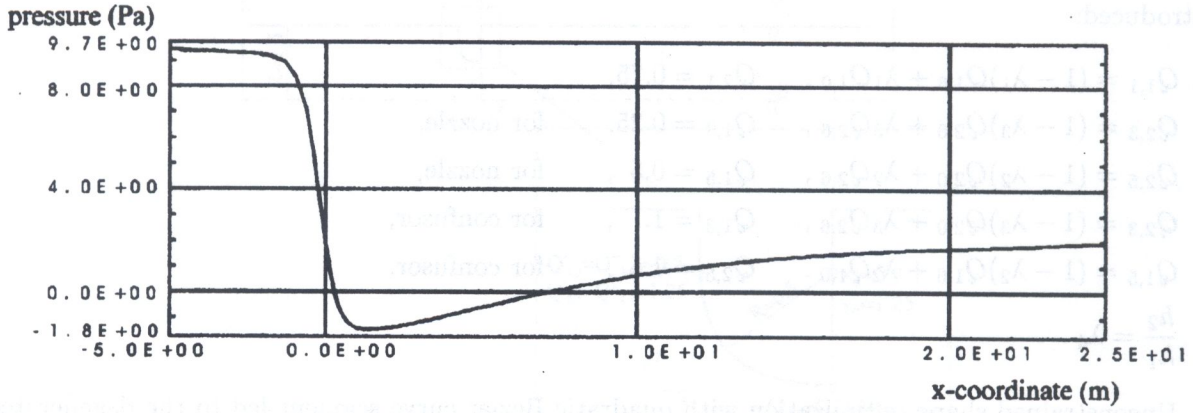

Fig. 5. Pressure plot on the axis

Table 2. The optimal confusor shape parameters (λ_i) and functional value e

λ_1	λ_2	λ_3	λ_4	e
1.0	0.16105	0.42076	1.03285	55.85

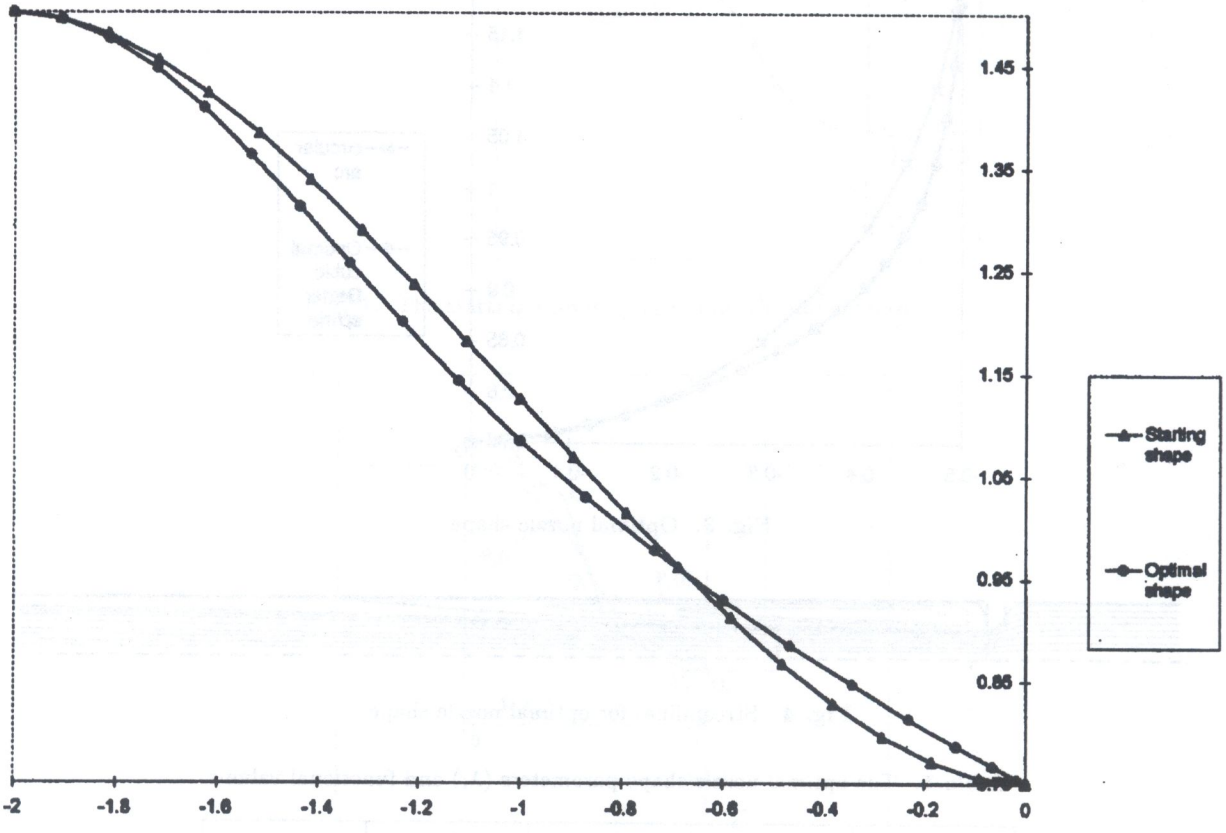

Fig. 6. Optimal confusor shape

The calculation was carried out using specially tailored mesh generator for the nozzle shape. The number of elements used in the calculation was 704 with 2253 nodes. In order to check the convergence mesh dependency, the calculations with finer mesh, 1008 elements with 3197 nodes, were carried out, showing very good agreement. Near optimum results were achieved after few iterations of conjugate gradient method, while for optimum result ten iterations on average were necessary.

In the case of the optimization of the confusor different confusor lengths were tested, since the losses are dependent on it. The one that is presented here has length to smaller diameter ratio equal 2 : 1.5. Here unconstrained optimization was adequate since all the parameters λ were in the interval $0, 1$. The number of Bezier cubic curve segments was two as in the nozzle case too. The optimal parameters are given in Table 2.

The starting and optimal shape of the confusor are shown in Fig. 6. Note that the vertical unit length is twice the horizontal.

7. Conclusion

The finite element incompressible viscous flow solver, with discretization of total derivative, was developed originally and has been tested on many test cases showing good convergence properties and robustness. Optimization with conjugate gradient method, with finite difference approximation of gradient of objective function and specially tailored mesh generator for chosen shape parametrization, has been successfully used. The optimal shape was searched for in the space of the splines made by cubic Bezier curve segments. Optimization with different initial values of parameters was carried out to test the convergence property. All solutions converged to the same result in ten iterations on average. The optimal shape for two cases: nozzle and confusor was calculated. All test cases showed good convergence properties what qualifies the proposed methodology as appropriate for shape optimization in viscous flow problems. The authors are developing the code for optimization of the nozzle shape for turbulent flow.

References

[1] G. Bugeda, E. Oñate, D. Joannas. Mesh adaptivity in shape optimization, application to incompressible potential flow. In: K. Morgan et al., eds., *Proceedings of VIII International Conference on Finite Elements in Fluids — New trends and applications.* J. Wiley, Barcelona, 1993.

[2] A. Dervieux. Some recent advances in optimal shape design for aeronautical flows. In: S. Wagner et al., eds., *Computational Fluid Dynamics '94,* 251–258. J. Wiley, Chichester, 1994.

[3] *DIN 1952, Durchflussmessung mit Blenden, Duesen, und Venturirohren in voll durchstroemten Rohren mit Kreisquerschnitt.* Beuth Verlag GmbH, Berlin, 1982.

[4] T. Fol, P. Colin, D. Destarac. Application of Numerical Optimization Methods to 3D Aerodynamic Design. In: S. Wagner et al., eds., *Computational Fluid Dynamics '94,* 259–267. J. Wiley, Chichester, 1994.

[5] L.D. Landau, E.M. Lifshic. *Teoretičeskaja fizika, tom VI, Gidrodinamika.* Nauka, Moskva 1988.

[6] Z. Mrša. Optimal design of spiral casing tongue and wicket gate angle by decomposition method. *Int. J. Num. Meth. Fluids,* **17**: 995–1002, 1993.

[7] Z. Mrša, Finite element modeling of laminar flow of incompressible viscous fluid with discretization of directional derivative. In: *Proceedings of the 1st Congress of Croatian Society for mechanics, Pula, Croatia,* 430–438, 1994.

[8] Z. Mrša, G. Medić. Optimal nozzle design using finite element conjugate gradient based software. In: *Proceedings of HYDROSOFT '96* (to appear).

[9] Z. Mrša, L. Sopta. Optimal shape design of Francis turbine spiral casing. In: K. Morgan et al., eds., *Proceedings of VIII International Conference on Finite Elements in Fluids — New trends and applications,* 1281–1289. J. Wiley, Barcelona, 1993.

[10] O. Pironneau. *Optimal shape design for elliptic systems.* Springer-Verlag, New York, 1984.

[11] O. Pironneau. *Finite element methods in fluids.* Masson, Paris, 1989.

[12] L. Sopta, Z. Mrša. Towards Complete Shape Optimization of Francis Turbine Spiral Casing. In: S. Wagner et al., eds., *Computational Fluid Dynamics '94,* 1025–1029. J. Wiley, Chichester, 1994.

[13] C. Taylor, T.G. Hughes. *Finite element programming in fluids.* Pineridge Press Ltd., Swansea, 1981.
[14] K. Weeber, S.R. Hoole. A structural mapping technique for geometric parametrization in the optimization of magnetic devices. *Int. J. Num. Meth. Engng.*, **33**: 2145–2179, 1992.
[15] F. Yamaguchi, *Curves and surfaces in computer aided geometric design.* Springer-Verlag, Berlin, 1988.